Planning of satellite images applied to early warning hydrological models

Estefanía De Elía, Marcelo Oglietti, Sergio Masuelli, Eduardo Romero
CONAE - Argentine National Space Agency
CETT, RP C45 Km 8, Córdoba
Argentina
{edeelia}{marcelo.oglietti}{sergio.masuelli}{eromero}@conae.gov.ar

Abstract.
Space information has become essential for assessing the damages caused by natural emergency situations like earthquakes, flooding or fires after its occurrence. During the last decade the effort increasingly moved to the objective of using operational systems that combine space information and physical modeling for forecasting and emergency mitigation action planning. These emergency early warning and mitigation support systems require as input space information of a higher quality like high resolution optical or synthetic aperture radar (SAR) images which are scarce resources and require an significant latency from request to the actual image acquisition.

In this paper we show that for the particular case of flooding it is possible to use a operational medium fidelity physics model to forecast the risk of flooding events and use this result to select in advance which are the most convenient images acquisitions to request for the near future. We briefly describe the Reduced Complexity Kinematic Wave Model used to predict potential flood events and the results demonstrate the model ability to replicate the process of runoff behavior over areas with little slope. We use this flood risk map prediction to give higher priority to those observations corresponding with areas of higher risk of flooding, to overcome usual earth observation satellite system reaction time constrains, implying that we can start acquiring useful data from the beginning of the flood event.

1 Introduction

During recent years, Earth Observation Satellites (EOS) space missions experienced an important increase both in number and complexity. The main objective behind several EOS missions currently under development it is not anymore just to provide data for the scientific community *post fact* analysis, but increasingly to develop *near real time* operational models and applications. Planning and scheduling of several EOS/sensors is an increasingly important problem for space missions because the need of guaranteeing an optimal use of its resources and a key factor for any near-real time operational application system.

This is particularly true for emergency management where currently there are several countries operating and developing space missions with this objective (e.g. Covello et al. (2010) and Wang et al. (2011)). Another interesting example of this operational applications approach for emergency is SensorWeb 2.0. Mandl et al. (2008) presents an ambitious space sensor web for disaster management with the objective of facilitate the United States contribution to the Global Earth Observation System of Systems (GEOSS). GEOSS is a worldwide initiative in this direction, with the objective to form a network of EOSs for a wide range of applications in order to provide a real-time picture of the whole planet by sharing all countries sensor resources. This sensor web relays on most important standards in the area like the Open Geospatial Consortium (OGC) and the Sensor Web Enablement (SWE) suite. SensorWeb 2.0 intents to present to the user the most simple possible experience integrating automatically several space, air and ground sensors, e.g. Moderate Resolution Imaging Spectrometer (MODIS), NASA's Earth Observing One (EO-1), the US's Air Force Weather Agency and an Unmanned Aerial System (UAS). The sensor web allows the users to define their regions of interests and then the system automatically detect events of interest. What the users wants to see is automatically executed by means of an appropriate workflow and the best available sensors. For example, if a fire is detected by inspecting MODIS data, this automatically triggers a higher resolution instrument like the Hyperion on the EO-1 satellite to take a higher resolution image, which in turn also automatically triggers an Unmanned Aerial System take for more detailed imagery.

An EOS system *response time* is all the time needed for an acquisition reception, scheduling, uplink, execution, data downlink, processing and distribution. EOS systems response time are considered one of the key variables for the success of these applications (Covello et al. (2010)). This is not surprising considering that an EOS system response time usually goes from 24 hours up to a week depending on the capabilities of the mission satellites and ground segment and that for several applications events of interest might have durations of a few hours or days. Being durations of comparable order of magnitude implies that even an small change in the response time might imply a difference in the feasibility of a particular operational application. Within the

emergency management context, time plays a major role and system response time becomes even more critical.

Often it is difficult to gather images of value corresponding to the first day of an emergency event since they are generally requested once the event has already occurred, meaning that we frequently lost the opportunity of having this very useful science data. Whenever possible, forecasting seems to be the only answer to this problem. In the particular case of flooding, it is rather possible to predict an event, allowing us to set up in advance future acquisitions of EOS images by determining which data is more convenient to acquire, and even, trigger also other air and ground systems activities, combining all this effectively.

This paper explores the use of forecasting of flooding and its use for the selection of which acquisitions are more convenient to schedule in order make more effective use of the space resources avoiding loosing the first hours/days of most critical data, particularly important for emergency applications. Using an operational medium fidelity physics model we generate a flood risk map prediction over the region of interest, which then is used to prioritize all possible future acquisitions. By given higher priority to those observations corresponding with areas of high risk of flooding, these acquisitions are selected and can be uploaded to the EOS, before the actual flood has even started. This overcomes the EOS system reaction time constrain and we might be able of start acquiring useful data just on time from the very beginning of the flood event.

The work presented here is considered a small step into the exploration of the vast world of possibilities that is the integrated use of early warning models in planning and scheduling, a promising path to build real life operational applications. We developed a simple planning system but complex enough to allow us to explore and share our main idea about how to use an early warning model continuous output for prioritizing future acquisitions requests that instead help improve the performance of the early warning model. It is worth underlining that this planning system is not the actual planning system of the EOS system we used, but instead it has the unique purpose of selecting which are the best acquisition to request for one application. Scaling this up goes first in the direction of running several applications like this in parallel, each selecting which are the best acquisitions for its own purposes. Furthermore, we consider that for arriving to successful real life operational applications the present approach shall be used in combination with several of the methods developed in the papers reviewed in the previous work section. For example, the quality of the predictions are important to avoid false positives that might push the system to acquiring data that is not the most critical. Medium fidelity models will certainly fail to capture the whole reality. Then, using an approach like that of Sensor-Web 2.0 EO-1/ASE it is very important in order to correct any false positive prediction as soon as possible.

The approach we present here can also be understood as a way of optimizing the EOS resources, by selectively deciding which products should be acquired it reduces the amount of unused data downloaded and processed.

Value-added and emergency space applications typically rely on a physical model of the phenomenon under study for which a reliable data source it is very important. During a flood event, we frequently also have a lot of cloud coverage, what makes the use of optical sensors more unreliable for this kind of emergencies. Instead, SAR images that are not affected by cloud coverage can be used to monitor and map the extent of flooding. That is why SAR images are increasingly used for emergency applications in order to gain in reliability and to get a response time as lower as possible.

We choose to work with the following two EOS missions with SAR instruments: Radarsat-2 and ALOS. The main RADARSAT-2 instrument is a SAR with quadri-polarization, very useful for flood events monitoring, designed with 10 modes of acquisition and offering a range of incidence angles allowing to choose the beam position with each mode. Each acquisition mode has a particular area coverage and spatial resolutions. The Satellite has a Synthetic Aperture Radar (SAR) with multiple polarization modes, including a fully polarimetric mode in which HH, HV, VV and VH polarized data are acquired. Its highest resolution is 1 m in Spotlight mode (3 m in Ultra Fine mode) with 100 m positional accuracy requirement. In ScanSAR Wide Beam mode the SAR has a nominal swath width of 500 km and an imaging resolution of 100 m. Its left looking capability allows the spacecraft the unique capability to image the Antarctic on a routine basis providing data in support of scientific research. ALOS has three instruments: L-band SAR, a panchromatic camera and a visible and near infrared radiometer. This selection allowed us to have in the model both optical images and radar images with different resolutions, coverages and acquisitions modes, and at the same we time keep the problem simple with only two satellites.

This work presents a decision-making tool that choose from potential acquisitions of satellite images those more convenient for a flood emergency event in the shortest time possible based on the forecast of a simple hydrological model. In what follows we present the hydrological model, the planning problem model and the integrated system developed.

2 Hydrological Model

The hydrological model is based on a reduced complexity kinematic wave model, i.e. we use a simplified equation of Saint-Venant (Neil M. et al., 2007)) that was implemented to identify possible areas affected by flood events. Since the first proposal by Zanobetti et al. (1970) methods for predicting plain flood by methods of storage cells have become justifiably popular. These methods discretize the floodplain according to a regular Cartesian (or raster) grid and each

floodplain pixel in the grid is then treated as an individual storage cell, with inter-cell fluxes calculate using uniform flow equations such as Manning. We assign to each cell an elevation equivalent to the average of all surveyed heights within the cell and its status within the grid is updated at each time step according to the input and output of the water flow. For many of these models the flow channel is calculated using the 1D Saint-Venant equation and when the flow overflows bankfull depth the water is directed to the storage cells of the floodplain (Paul D. et al., 2010). Hydraulic models can be classified according to the number of dimensions in which they represent the spatial domain and flow processes therein, and for particular problems a one-, two- or even three-dimensional model may be most appropriate

For channel flow below bankfull depth there is increasingly a consensus (after Knight and Shiono (1996)) that flow processes can be adequately described by some form of the one-dimensional shallow water equations. When a flood occurs, channel flow overflows bankfull depth and water spills onto adjacent floodplains with smaller slope. This situation becomes much more complex and can not be satisfactorily represented by simple dimensional schemes (Neil M. et al., 2005). Although 1D codes are computationally very efficient they suffer from a number of drawbacks when applied to floodplain flows. These include the inability to simulate lateral diffusion of the flood wave, the discretization of topography as cross sections rather than as a surface and the subjectivity of cross-section location and orientation (Samuels, 1990). All of these fundamental constraints can be overcome with two-dimensional codes and numerous classes of 2D schemes have been developed in response.

The aim of developing and using models that are "as realistic as possible" must be balanced against a number of other important considerations (Beven, 2001) like: the computational burden of the hydrodynamic model, investment in data collection and model set-up and maintenance. Therefore, the choice of appropriate flood model (diffusive wave or kinematic wave Saint-Venant, 1D or 2D, etc) does not only depends on the terms that may be omitted from the Saint-Venant equation. The availability and accuracy of the input data, such as topography, hydraulic properties of the river and the floodplain and upstream and downstream hydrographs is critical information.

Specification. The channel flow (river) is modeled with a kinematic dimensional approach which is able to capture the flood wave propagating downstream and the flow response to free surface height. The model used in this work is based on the model LISFLOOD-FP, originally developed by Bates and De Roo in 2000 (Bates and De Roo, 2000).

This can be described in terms of continuity and momentum equations as:

$$\frac{\partial Q}{\partial x} + \frac{\partial A}{\partial t} = q \tag{1}$$

$$S_0 - \frac{n^2 Q^2 P^{4/3}}{A^{10/3}} = 0 \tag{2}$$

Where Q is the flow in the channel, A is the cross sectional area of flow, q is the water input from others sources, S_0 slope of the river bed, n is the GaucklerManning coefficient and P is wetted perimeter.

The floodplain flows are described similarly in terms of continuity and momentum equations, discretized on a grid of square cells that allows to represent fields of 2D dynamic flow on the floodplain. We assume that the flow between two cells is simply a function of the height difference between the free surface (Estrela & Quintas, 1994), see Figure 1:

$$\frac{dh^{i,j}}{dt} = \frac{Q_x^{i-1,j} - Q_x^{i,j} + Q_y^{i,j-1} - Q_y^{i,j}}{\Delta x \Delta y} \tag{3}$$

$$Q_{x,y}^{i,j} = \frac{h_{flow}^{5/3}}{n} \frac{(h^{i-1,j} - h^{i,j})^{1/2}}{\Delta x} \Delta y \tag{4}$$

Where $h^{i,j}$ is the height of free water surface at node (i, j), t is time, Δx and Δy are the grid cell dimensions, n is Manning's roughness coefficient of foodplain, Q_x and Q_y describe the volumetric flow rates (either positive or negative) between adjacent floodplain cells in the x and y Cartesian directions respectively and h_{flow} represents the depth through which water can flow between two cells.

Equation 4 is also used to calculate flows between cells of the floodplain and the channel, updating plain cells depths using equation 3 in response to the channel flow. These flows are used also as the source term in equation 1 linking channel and plain flows

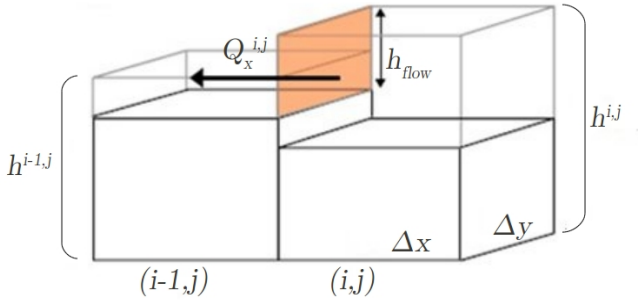

Figure 1: Flow at cell edge is determined by water height difference with adjacent cell

3 Planning Problem Model

The output of the hydrological model presented above is used as input for the image acquisition planning problem we describe here in order to request the most useful acquisitions. The planning domains and problems were specified in PDDL. For planning we uses best-first search algorithms and we implement a multi-objective metric that allowed us to

compare different solutions to the same problem according to different parameters. The algorithm showed good performance and found an optimal solution for each experimental test.

We divide the acquisition images planning problem in one slot per day. The duration of the planning time horizon for a single run is 24hs. We start solving the planning problem for the first 24hs, then we move to the next 24hs, and we continue like this repeating the planning cycle. In our model we use the natural variable D to define which is the current day over which we are planning. We increase it by one each day.

The process followed for planning each day has two phases: First, using a satellite sensor track propagation tool we generate the set with all candidates images, and second, using a planning tool we select the images to be requested on that day.

The satellite sensor track propagation tool task is, given the valid EOS ephemerids for day D and all valid target areas, to propagate the sensor swath projection on ground and to identify all possible candidate images on day by registering the start and end time of each intersections between the sensor swath and the areas corresponding to the referred user requests. This shall be done for each sensor mode because the swath of each mode is different. The planning tool task is to generate the choose from the set of candidate images those that maximize the quality of the acquisition plan.

We consider that the details related with the use of the satellite sensor track propagation tool are not interesting, and correspondingly, in what follows we focus in the modeling does for the planning tool.

3.1 Specification

Users does not request images directly. Instead, their requests are usually defined by what is more close to their needs. In our model an *acquisition request* is defined by: (a) a target area definition, (b) an acquisition mode preference definition stating what modes are more useful for the user, (c) the priority that defines the importance of the request for the user, and (d) a validity period within which the acquisition is useful. We denote by $R(D)$ the set of all valid users acquisition requests for day D (i.e. which validity period includes D). For any $r \in R(D)$ we denote by a_r its the target area definition, by mp_r its acquisition mode preference definition, by pr_r its priority and by v_r its validity period. We use R instead of $R(D)$ when this does not leads to ambiguity.

We encode in a single natural variable named *acquisition mode* all high-level configuration and constraints options that a user can choose when requesting an acquisition. For example, if the EOS has two possible nominal incidence angles for any acquisition, two operational modes and three possible polarizations, we will encode all twelve possibilities a $\{1, ..., 12\}$. For each EOS we define the set $M = \{1, ..., k\}$ that encodes all its possible acquisition modes. An acquisition mode preference definition mp_r is a function $M \longrightarrow MP$ that associates to each element in M a value in $MP = \{1, ..., n\}$ a subset of the natural numbers that is used to define the user preference for each particular mode, being 1 the maximum preference and n its minimum . For example: If an EOS has only three acquisitions modes and if an user request has the highest preference for mode 2, four time less preference for mode 3 and several times less preference for mode 1, we can model this with $M = \{1, 2, 3\}$, $MP = \{1, ..., 100\}$ and $mp_r = \{(1, 100), (2, 1), (3, 4)\}$.

An EOS usually has several operational constraints that derive from its thermal, power, memory storage, communication and instrument operation capabilities and limits. From the point of view of the elaboration of a plan of acquisitions, it is frequently possible to translate this set of physical constraints into a set of temporal constraints over the various images that can be taken. For example, as limits to (a) the total amount of time that the instrument can be acquiring images per orbit, (b) the amount of time between two successive acquisitions what usually depend on the acquisition mode, and (c) the amount of time that the instrument can be continuously acquiring an image (may be different for the acquisition mode).

These temporal constraints on acquisitions can be divided as follows: (a) constraints over any number of acquisitions but over a period of time, like per day or per orbit, (b) constraints over two contiguous acquisitions, and (c) constraints over a single acquisition. For simplicity, the model we are presenting here only considers the case (b) of constraints over pairs acquisitions.

We assume that EOS acquired images are restricted to be rectangular strips, which width depends on the acquisition mode and which length it is given by the duration of the acquisition. Even if in general other kind of images might be taken, most EOSs in nominal conditions operates in agreement with this assumption. Here we refer by *candidate image* to a possible single image acquisition that at least partially covers one single user acquisition request r for some mode. We denote by $I(D)$ the set of all candidate images within the planning time horizon corresponding to day D. We use I for $I(D)$ whenever this does not lead to ambiguity. Notice that I includes all the images corresponding to all possible modes of acquisitions in M and each image $i \in I$ is a member of the set because it covers partially at least one user acquisition request r. Given a user acquisition request $r \in R$, we denote by I_r the subset of I with all possible candidate images that are present in I because they cover partially the target area of the acquisition request $r \in R$, i.e. of a_r. Notice that $I = \bigcup_{r \in R} I_r$.

Given a valid acquisition request $r \in R$, for any $i \in I_r$:

- ca_i denotes the *covered area* of i defined as the percentage

of the acquisition request target area a_r that is covered by the image i (with values from 0 to 1);

- md_i denotes the *mode* of i defined as the mode $md_i \in M$ corresponding to image i acquisition;
- ma_i denotes the *mode adequacy* of i defined as $ma_i = mp_r(md_i)/k$ where $k = |M|$, i.e. the preference value mp_r corresponding to the mode md_i of i over the maximum mode preference value k (with values from 0 to 1);
- pr_i denotes the *priority* of i defined as $pr_i = pr_r$, the priority we assigns to image i is the priority defined by the user acquisition request r (values from 0 to 1);
- us_i denotes the *used swath* of i defined as the percentage of the swath that goes over the target area a_r, (values from 0 to 1);
- $[st_i, et_i]$ denotes the *time window* of i with a st_i start time and a et_i end time.

The planning problem is assumed oversubscribed, and correspondingly, only a subset of $I(D)$ can be actually selected to be requested per day. We denote $SI(D)$ the subset of $I(D)$ with all *selected images* to be requested for day D. We use SI for $SI(D)$ whenever this does not lead to confusion.

Notice that I is the input for the planning tool and that SI is its output, i.e. the planning tool task is to generate the set SI by selecting from the set I of candidate images those that maximize the quality of the acquisition plan.

Temporal Constraint. As mentioned above the present model only considers the case of constraints over pairs of consecutive acquisitions. For each pair of images $(i, j) \in I \times I$, we denoted by tt_{ij} the minimum transition time the satellite needed between the end of an acquisition i and the start of acquisition j. We include in tt_{ij} all sources, from slew time to acquisition mode change durations. For simplicity, we considered the minimum transition time as depending only on the acquisition modes of both i and j images (i.e. on md_i and md_j) and we assign $tt_{ij} = 0$ when $i = j$ and $tt_{ij} = tt_{ji}$, (even if in the latter case we could have help eliminate several cases by setting $tt_{ij} = INF$ whenever $i > j$).

Given a subset of I denoted by S, we said that S is a *feasible solution* that satisfy all temporal constraints when for any pair $(i, j) \in S \times S$ we have that $et_i + tt_{ij} < st_j$ or $et_j + tt_{ji} < st_i$. We denote by $DI(D)$ the subset of I with all *discarded images* those images that if added to S make the set not a feasible solution. We write simply DI instead of $DI(D)$ when it is not ambiguous.

Objective Function. The set SI is the feasible solution S that maximizes the quality of the acquisition plan. By combining four terms with α, β, δ and σ non-negative constants that are used in order to give different weight them we define the following objective function such that the feasible solution that minimizes it is the optimal solution:

$$F(S) = \alpha f_{ca}(S) + \beta f_{pa}(S) + \delta f_{ma}(S) + \sigma f_{us}(S) \quad (5)$$

with:

$$f_{ca} = \sum_{i \in S} 1 - ca_i \quad (6)$$

f_{ca} measures the quality of the solution regarding total covered area. f_{ca} is optimal when an acquisition covers a wide part of a region of interest (near 100%), ie the value of ca_i is high and the total value $1 - ca_i$ is low. As the optimal solution minimizes the function f_{ca}, acquisition i becomes a good candidate to be selected by the planner.

$$f_{pa} = \sum_{i \in S} \frac{pr_i * (1 - ca_i + 1)}{2} \quad (7)$$

f_{pa} measures the quality of the solution regarding areas with greater priority. f_{pa} is like f_{ca} with the difference that the percentage value of area covered by acquisition is weighted by the priority of the associated region. When area coverage of two or more acquisitions is equal or similar, the value pr_i will decide which image select. The image with less chance of being selected is one that covers a small percentage of an area and the priority of the region associated is very low (equivalent to high values of pr_i).

$$f_{ma} = \sum_{i \in S} \frac{ma_i}{k} \quad (8)$$

where $k = |MP|$ is the cardinality of MP, the value that correspond to the lowest preference. f_{ma} measures the quality of the solution regarding the acquisition mode adequacy. f_{ma} considers the priority of an acquisition mode, depending on whether an appropriate mode to monitor a particular emergency. In the worst case $\frac{ma_i}{k}$ equals 1, i.e. ma_i equals k , this would indicate that the acquisition mode of i is not the most appropriate and therefore it has a low priority assigned. In the best case, the most appropriate mode has priority equal to 1 and the fraction $\frac{ma_i}{k}$ reaches the smallest value possible

$$f_{us} = \sum_{i \in S} 1 - us_i \quad (9)$$

f_{us} measures the quality of the solution regarding swath percentage over the area of interest. A optimization criterion can be evaluated where the main interest is focused on maximize the use of the sensor instead to monitor an area. This idea aims to satisfy various user requests with a single satellite pass. The optimal case of the function f_{us} occurs when the value of swath percentage us_i used to cover an area is high and the total value $1 - us_i$ is low.

3.2 Implementation

Planner tool. Even if we could had used a different approach to solve this optimization problem, we preferred to use a planning tool and a domain independent language for modeling the problem, because the purpose behind this work is to start gathering experience with the main idea of integrate with synergy both the simplified application model and a planning tool with the purpose of optimize the space resources.

There are several planners able to solve classical planning problems, but only a few support metrics. We choose to work with the planner Metric-ff (Hoffman, 2003) and use its WA* search algorithm. The WA* is an algorithm of *Best-First Search* type and it is based on the same principles as the A* algorithm. The best-first search select a node for the expansion based on an evaluation function $f(n)$ with the lowest evaluation. $f(n)$ evaluates each node by combining the cost to reach a node n ($g(n)$) and the cost to reach the target node ($h(n)$ - heuristic): therefore $f(n) = g(n)+h(n)$ gives the estimated lower cost of the solution through n node. WA* adds a weight to each parts of the evaluation function (heuristic and cost). We defined both wh and wg equal to 1 respectively. The $g(n)$ we use is $F(S)$ the objective function we presented in previous section.

Space State and Initial state. In our model the space state is defined simply by $SI \cup DI$. To obtain the initial set of images on a given area the SaVoir software was used for given each satellite orbit, the sensor geometry and the shape and location of the user's acquisition request target areas, to determine exactly when a satellite is start and end observing the target. The initial state of each planning problem specified in PDDL was create by running a tool that takes the XML output file of SaVoir software and convert it to the PDDL input for the planner.

Planning domain definition. The domain and planning problem were specified in PDDL v2.1 (see (Fox and Long, 2003)). PDDL object types, functions and predicates were specified as follows. Four objects were defined: (a) image: representing each candidate image; (b) mode: representing the various modes in M; (c) area: representing an acquisition request target area; and (d) D: representing current day. For simplicity, we abstract here that indeed mode was represented with two objects that decompose mode in two fields mainMode and subMode.

Six predicates and seventeen functions (fluents) were specified. The figure 2 shows the two possible states where both images may be acquired. These situations are similar but they show that the order of acquisitions should be considered. Because the planner selects an image depending on the evaluation function we need to look forward and back over the planning horizon. Otherwise if in the case 2 b. the planner first selects the B image then we would lose the A image

Seven actions were needed: one for choosing the first image when no image is in SI, two more for selecting an image in the two conditions shown in figure 2, and four more for discarding an image in the four conditions shown in figure 3.

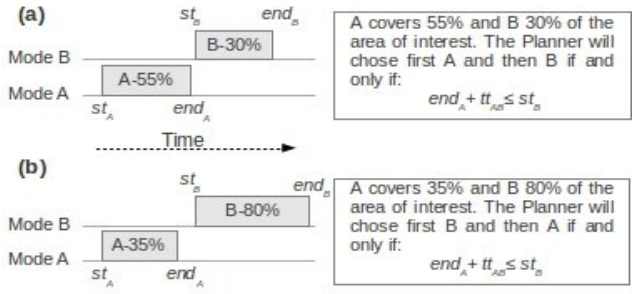

Figure 2: States where is possible to acquire both image

The figures 3 show four situations where a temporal conflict occurs between the images acquisitions.

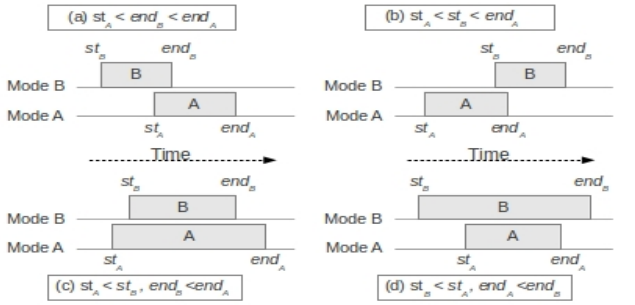

Figure 3: States where is not possible to acquire both image

Goal. We model the on board memory storage capacity, communication down link capacity and ground segment operational capacity by limiting the total number of images that can be selected per day to be less than mm, i.e. $|SI| \leq mm$. Correspondingly, the planner will terminate when the number of images in SI equals mm or because all the images in I are selected or discarded (i.e. $SI \cup DI = I$). We refer the former case as *bounded goal*, the latter as *unbounded*, and that an image is *checked* if it is in $SI \cup DI$.

3.3 Tests and results

Table 1 shows the results obtained with the planner for four scenarios described below. For scenario A, D and C we used unbound goals and for scenario D we used a bounded goal limiting the images in SI to a maximum of 6.

A. Four acquisition modes (EH2, EH4, EH6 and F6N of SAR sensor on board RADARSAT-2 satellite), planning 4 days, the region of interest the low basin of Bermejo river was visualized by the sensor two days, and an unbounded goal;

Scheduled images	Selected images	Visited nodes	Time	Metric	Scenarios
8	3	48	0.47"	f_{ca}	A
8	2	52	0.62"	f_{ma}	A
8	3	48	0.47"	$f_{ca}+f_{ma}$	A
8	3	48	0.31"	f_{us}	A
12	4	2976	2.96"	f_{pa}	B
18	9	867	22.15"	f_{ca}	C
18	6	95	19.19"	f_{ca}	D

Table 1: Comparative table of tests and results

B. Acquisition modes like in item A, planning 4 days, the region of interest the low, middle and high basin (each with different observation priority) of Bermejo river visualized by the sensor three days, and an unbounded goal;

C. Seven acquisition modes (one mode of AVNIR-2 sensor on board ALOS satellite, two modes of PALSAR sensor on board ALOS satellite and four modes of SAR sensor on board RADARSAT-2 satellite), planning 4 days, the region of interest the low basin of Bermejo river was visualized by the sensors everyday, and an unbounded goal;

D. Everything like in point C, but with a bounded goal limiting images in SI to a maximum of 6.

4 Integrated System

The figure 4 shows the architecture of the integrated system, its main subsystems and interfaces, and some key units.

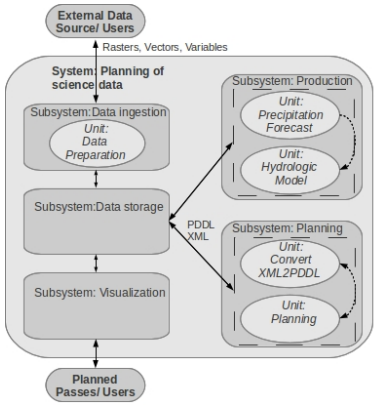

Figure 4: Architecture of integrated system

Five main modules were considered:

- Data ingestion subsystem (SI): the external interface used for receiving the input data, process and store them. This subsystem can be composed of one or more units responsible of processing and manipulating data. According to our system, this unit receives the input data from the hydrological model, e.g. precipitation layer or a Digital Elevation Model;
- Data storage subsystem (SA): interacts with all the subsystem and it manages its data. The communication between units is done through this subsystem and therefore changes on one module are transparent to the rest;
- Production subsystem (SP): This unit generates the data tuple *(region, time)*. It has two main units, the first unit is responsible to obtain automatically a forecast of rainfall. The second unit implements the hydrological model, it obtains the input data from SA subsystem and then stores its output there;
- Planning Subsystem (SPLA): This subsystem plans the set of acquisitions. We consider two main units, the first translates from XML (format of SaVoir output files) to PDDL. The second unit refers to the Metric-FF planner used;
- Display Subsystem (SVI): Currently this subsystem is represented by SaVoir software with which we visualize the input variables to the planner and the output selected images.

One integrated scenario

A test scenario was created. The hydrological model was ran on Bermejo River basin, located north of Argentina. For a time window equal to seven days two overflow regions were forecasted for the model. Because the overflow areas are narrow regions, it was worked with *Ultrafine* and *Fine* modes of SAR sensor onboard Radarsat satellite whose spatial resolutions are the highest offered by the instrument, 3m and 8m respectively. For a planning of seven days on regions of interest 13 images were identified as potential acquisitions (figure 5)

Figure 5: Gantt Chart: potential acquisitions on critical regions

The planner found a solution in 40 seconds and went through 30782 nodes and the plan was evaluated according

the total of covered area by each image and its acquisition mode. The first overflow area occurs between the first and second day of simulation and the second overflow area occurs during the fifth and sixth days of simulation. Therefore, the selected images on the first region during the first days will provide important information about the start of the flood. On the other hand the selected acquisitions these days on the second region will provide information before the event, which are useful for further studies. A similar situation happens with selected images during the last days, they will provide post-event information on the first region and current information on second region. Figure 6 shows the obtained results, where five images were selected according to the established metric.

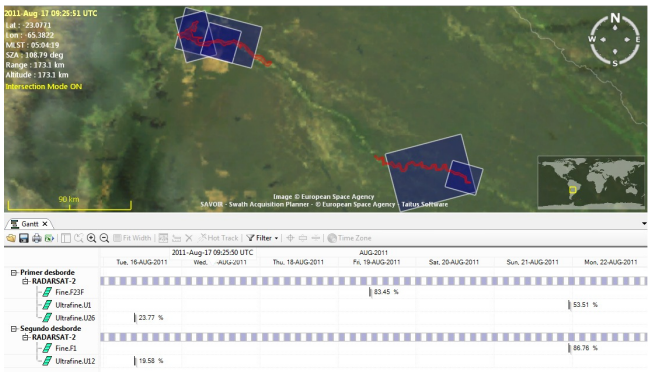

Figure 6: Map and Gantt chart of the selected images on the critical regions

The final selection was varied, in some cases the total of covered area was prioritized and other cases the acquisition mode was prioritized. For example, for the first day of planning on the second region of interest the image *Ultrafine.U12* with more resolution was selected. Otherwise for the fourth and sixth day the opposite happened. While *Ultrafine* mode has a higher priority that *Fine* mode, this last was selected because its percentage of area covered is higher.

4.1 Related work

Frank et al. (2001) address the problem of scheduling observations for a collection of EOS solving the scheduling problem by means of an stochastic greedy algorithm. (Bianchesi and Righini, 2008) also address this problem adding also the transmission of images and needed contact with earth stations. Lemaitre et al. (2002) illustrated several algorithmic techniques for planning and scheduling problems of the Pleiades constellation.

Globus et al. (2003) presented a genetic algorithm to a problem with two satellites in a short planning horizon, without memory and transmission constraints. Problems with one satellite were also studied by Wolfe and Sorensen (2000) and by J.F. and G. (2005) who solved small instances with number of 50 requests. Bensana et al. (1999) y Vasquez and Hao (2001) considered the problem of scheduling of one optical satellite. SAR instrument scheduling was considered by Harrison et al. (1999), who resolved cases with a single satellite, 50 requests and a time horizon of a few minutes.

Potter and Gasch (1998) considered the problem of scheduling Landsat7 mission daily activities by selecting the requests with highest priority. The priority of each request is continuously adjusted by considering a multi-factor criteria including cloud covering, age of request, risk of a unfulfilled request, seasonal/latitude characteristics and clustering. Even if the approach is driven by the received scene requests this continuous priority adjustments allows to dynamically adjust the scheduling based on all key dynamical factors improving overall plan quality.

Chien et al. (2005b) and Chien et al. (2005a) presents a very successful project developed for EO-1 mission flight an Autonomous Sciencecraft Experiment (ASE) that uses dedicated autonomy flight software to improve science return for various applications (e.g. wild fire and floods management). Starting from a ground defined and up-linked set of high-level goals (regions of interest), on board software, named classifiers, analyze the images and when new activity is detected, more detail science goals are generated to continue monitoring the site. If no activity is observed, the image is not down-linked saving costly mission resources.

Ip et al. (2005) present in more detail the advantages of ASE for floods management applications, showing how it effectively improves communication latency and bandwidth restrictions, increase science content returned data by filtering unuseful data such as scenes covered by clouds, identifies science features of interest such as flood-induced change and automatically re-plan on-board science goals triggering the recollection of interesting data when a change is detected. By placing data analysis and decision making on-board the spacecraft, ASE reduces the time it takes to detect and react to a flooding event to a few hours autonomously. ASE flood *classifiers* demonstrated their ability to accurately detect on-board various types of floodwaters, allowing a rapid response on the onset of flooding and correspondingly to increase the return of data of greatest value.

Chien et al. (2011) present a pilot operational flood management application developed for monitoring Thailand floods regions. This application uses several space data sources and a sensor web, (including SAR satellite data as we do in the present work). In this application the earliest flood detection is done on ground by using MODIS data. When a flood is detected, a specific goal is automatically generated and uplink to EO-1 satellite that after pursue related floods data using its on board autonomous capabilities. When needed more low resolution optical or SAR imagery is automatically requested from various satellites (e.g. worldview, Ikonos, radarsat2). Finally, from surface water extent

and a digital elevation model a water volume product is automatically generated.

Summarizing: Until recently, the starting point for most space systems activity was given by a series of acquisition requests generated outside the system by its end users, e.g. the scientific community. Correspondingly, planning these space systems activity was in practice reduced to scheduling this oversubscribed acquisitions requests. EO-1 ASE proposed an alternative scheme: on-board, its various *classifiers* analyze science data in near real time. When an event of interest is detected, triggers the generation of a new goal and re-planning of the sensor acquisitions: ASE starts scheduling all convenient future science acquisitions related with the event. This scheme shortens the response time period between the start of the event of interest and when the system starts acquiring useful data. This is valid only for certain regions of interest that are specified as high-level goals over which the *classifiers* are run. SensorWeb 2.0 add to this scheme the possibility of automatically analyze one sensor data at ground and use this to automatically trigger requests of other sensors acquisitions. For example, the approach followed in Chien et al. (2011) use MODIS data analysis in order to detect a flood condition. When this occurs, a lower resolution EO-1 acquisitions is automatically generated.

Optimizing which acquisitions are more convenient considering both predicted and current flood at the same level is a broader planning problem, in the sense that it requires incorporating early warning models into the planning loop.

5 Future work

There is place for improvement in relation to current application and also to work on a similar scheme but with other applications like wild fire management, or malaria and dengue fever control. We are planning to work in enrich the image acquisition planning model, tools and algorithms used in several aspects like: (a) to consider constraints on the number of acquisitions for a given period of time (e.g. by orbit) and constraints over single acquisitions (e.g. cannot take images continuously by more than 10 minutes) and other constraints that reflect better ground, satellite and communications limitations; (b) to automatically cut all parts of a user request target area when acquired in order to pass to the next planning cycle only the uncovered parts of that area; (c) to test different algorithms for the optimization problem, including tuning differently current one; and (d) to use planing and scheduler tools that allows a better temporal representation.

Our final objective is to put in place various operational hydrological applications of emergency management for various flood basins over Argentina to be used in the context of CONAE's SAOCOM mission, such that each one will allow us to request the images more convenient for each basin in agreement with the quota assignment.

6 Conclusions

The simplified wave hydrological model implemented predicts the affected areas and provides information about the movement of the flood wavefront that progresses downstream. This helps optimize the response time on the forecasts of flood events. We showed the model ability to replicate the process of runoff behavior on areas with little slope. The model showed good numerical stability taking into account hydraulic principles such as mass conservation and flow connectivity.

The image acquisition planning system we developed based on the planning domain and problem models described above shows that it is possible with available tools (like SaVoir and the Metric-ff planner) to use the hydrological model flood risk predictions to prioritize the acquisition image planning problem and determine which are the most useful image acquisitions that we should request for this particular application. The approach developed overcomes the EOS system reaction time constrains allowing us to start acquiring useful data just when it is needed, even before the actual start of the flood event.

The experimental evaluations of the planning system confirm that the time needed for solving the problem depends critically on the size of the initial state and that using a bounded goal help decreasing the time needed for solving the problem. If the number of images is not limited by a bounded goal then all images should be checked and therefore the response time varies according to the initial number of potential acquisitions and with the present approach the planning system eventually will stop converging to a solution in a reasonable time and with reasonable computer resources. The rationale behind the bound goal scheme is basically to limit the number of images that can be requested to the quota assigned to the application. This is based in the fact that SAR EOSs mission usually use a quota scheme: for each user/application –like the one presented here– a fix number of images, named quota, per period limit is assigned. The response time depends on the metric used and when the evaluation function combines two parameters like the percentage of covered area plus the priority acquisition mode the time needed is reduced.

References

Bates, P. and De Roo, A. (2000). A simple raster-based model for flood inundation simulation. *Journal of Hydrology 236*, 236:54–77.

Bensana, E., Lemaitre, M., and G., V. (1999). Earth observation satellite management. *Constraints*, 4:293–299.

Beven, K. (2001). How far can we go in distributed hydrological modelling? *Hydrology and Earth System Sciences*, 5(1):1–12.

Bianchesi, N. and Righini, G. (2008). Planning and scheduling algoritmos for the cosmo-skymed constellation. *Aerospace Science and Technology*, 12:535–544.

Chien, S., Cichy, B., Davies, A., Tran, D., Rabideau, G., Castao, R., Sherwood, R., Mandl, D., Frye, S., Shulman, S., Jones, J.,

and Grosvenor, S. (2005a). An autonomous earth-observing sensorweb. *Intelligent Systems, IEEE*.

Chien, S., Doubleday, J., Mclaren, D., Tran, D., Tanpipat, V., Chitradon, R., Boonya-aroonnet, S., Thanapakpawin, P., Khunboa, C., Leelapatra, W., Plermkamon, V., Raghavendra, C., and Mandl, D. (2011). Combining space-based and in-situ measurements to track flooding in thailand. In *Geoscience and Remote Sensing Symposium (IGARSS), 2011 IEEE International*, pages 3935–3938.

Chien, S., Sherwood, R., Tran, D., Cichy, B., Rabideau, G., Castano, R., Davis, A., Mandl, D., Frye, S., Trout, B., and Shulman, S. (2005b). Using autonomy flight software to improve science return on earth observing one. *Journal of Aerospace Computing, Information and Communication*, 2:196–216.

Covello, F., Battazza, F., Coletta, A., Lopinto, E., Fiorentino, C., Pietranera, L., Valentini, G., and Zoffoli, S. (2010). Cosmoskymed an existing opportunity for observing the earth. *Journal of Geodynamics*.

Fox, M. and Long, D. (2003). Pddl2.1: An extension to pddl for expressing temporal planning domains. *Journal of Artificial Intelligence Research (JAIR)*, 20:61–124.

Frank, J., Jonsson, A., Morris, R., and Smith, D. (2001). Planning and scheduling for fleets of earth observing satellites. *6th International Symposium on A.I., Robotics and Automation for Space*.

Globus, A., Crawford, J., Lohn, J., and Pryor, A. (2003). Scheduling earth observing satellites with evolutionary algorithms. *International Conference on Space Mission Challenges for Information Technology (SMC-IT)*.

Harrison, S., Price, M., and Philpott, M. (1999). Task scheduling for satellite based imagery. *PLANSIG99, 18th Workshop of the U.K. Planning and Scheduling Special Interest Group*.

Hoffman, J. (2003). The metric-ff planning system: Translating "ignoring delete lists" to numeric state variables. *Journal of Artificial Intelligence Research*, 20.

Ip, F., Dohm, J. M., Baker, V. R., Doggett, T., Davies, A. G., Castano, R., Chien, S., Cichy, B., Greeley, R., and Sherwood, R. (2005). Development and testing of the autonomous spacecraft experiment (ase) floodwater classifiers: Real-time smart reconnaissance of transient flooding. *Journal of Remote Sensing of Environment*.

J.F., C. and G., L. (2005). Maximizing the value of an earth observation satellite orbit. *Journal of the Operational Research Society*, 56:962–968.

Knight, D. and Shiono, K. (1996). River channel and floodplain hydraulics. *In: Anderson, M.G., Walling, D.E., Bates, P.D. (Eds.), Floodplain Processes. Wiley, Chichester*, pages 139–182.

Lemaitre, M., Verfaillie, G., Jouhaud, F., Lachiver, J., and Bataille, N. (2002). Selecting and scheduling observations of agile satellites. *Aerospace Science and Technology*, 6:367–381.

Mandl, D., Sohlberg, R., Justice, C., Ungar, S., Ames, T., Frye, S., Chien, S., Tran, D., Cappelaere, P., Sullivan, D., and Ambrosia, V. (2008). A space-based sensor web for disaster management. In *In Geoscience and Remote Sensing Symposium. IGARSS 2008. IEEE International*.

Neil M., H., Matthew S., H., Paul D., B., Matthew D., W., and Micha G.F., W. (2005). An adaptive time step solution for raster-based storage cell modelling of floodplain inundation. *Advances in Water Resources*, 28:975–991.

Neil M., H., Paul D., B., Matthew S., H., and Matthew D., W. (2007). Simple spatially-distributed models for predicting flood inundation: A review. *Science Direct, Geomorphology 90*, 387:208–225.

Paul D., B., Matthew, S. H., and Timothy, J. F. (2010). A simple inertial formulation of the shallow water equations for efficient two-dimensional flood inundation modelling. *Journal of Hydrology*, 387:33–45.

Potter, J. and Gasch, J. (1998). A photo album of earth: Scheduling landsat 7 mission daily activities. In *Proceedings of the International Symposium on Space Mission Operations and Ground Data Systems*, volume Tokyo, Japan.

Samuels, P. (1990). Cross-section location in 1-d models. *2nd International Conference on River Flood Hydraulics. Wiley, Chichester*, pages 339–350.

Vasquez, M. and Hao, J. (2001). A logic-constrained knapsack formulation and a tabu algorithm for the daily photograph scheduling of an earth observation satellite. *Journal of Computational Optimization and Applications*, 6:137–157.

Wang, P., Reinelt, G., Gao, P., and Tan, Y. (2011). A model, a heuristic and a decision support system to solve the scheduling problem of an earth observing satellite constellation. *Computers & Industrial Engineering*.

Wolfe, W. and Sorensen, S. (2000). Sorensen, three scheduling algorithms applied to the earth observing systems domain. *Management Science*, 46:148–168.

Zanobetti, D., Longer, H., Preissmann, A., and Cunge, J. (1970). Mekong delta mathematical model program construction. *American Society of Civil Engineers, Journal of the Waterways and Harbors Division*, 96 (WW2):181–199.